JCTC Journal of Chemical Theory and Computation

Charge Transfer Across ONIOM QM:QM Boundaries: The Impact of Model System Preparation

Nicholas J. Mayhall and Krishnan Raghavachari*

Department of Chemistry, Indiana University, 800 E. Kirkwood Avenue, Bloomington, Indiana 47405

Received July 24, 2010

Abstract: The inability to describe charge redistribution from regions I to II at the high level of theory imposes limitations on the general applicability of the our own N-layered integrated molecular orbital and molecular mechanics (ONIOM) method. In this report, we exploit the most inexpensive components of an ONIOM QM:QM calculation to provide a new method which has the ability to describe such charge-transfer effects with only a nominal increase in computational effort. Central to this method is the model system preparation step, in which an one-electron potential is optimized to shift density into or out of a defined buffer region. In this initial effort, we treat the link atoms on the model subsystem as the electron buffer region and swell or diminish the link-atom nuclear charges to shift electron density into or out of the buffer region. Due to the relatively small computational cost of the model-low calculation, this procedure can be iteratively optimized to produce a charge distribution equal to the real-low calculation. Initial results for a test set of 20 reaction energies and 8 different combinations of high and low levels of theory show improvements of more than 35% over the standard ONIOM QM:QM approach, with improvements of up to 50% for some high and low combinations.

1. Introduction

The steep scaling of computational cost with molecular size restricts application of the most accurate quantum chemical methods to relatively small molecules.[1−6] More approximate methods, while applicable to much larger chemical systems, often fail to achieve the accuracy required to obtain qualitatively correct results. One of the most popular approaches aimed at achieving a better balance of efficiency and accuracy has been through the use of hybrid energy methods.[7−16] By restricting expensive calculations to only the chemically interesting regions of a large molecule, hybrid methods try to combine accuracy and efficiency to extend the range of systems able to be treated computationally. To perform a hybrid energy calculation, the chemical system is first partitioned into different regions, and in the simplest case, two regions, I and II. The energy is then defined as

$$E_{\text{hybrid}} = E(\text{I}) + E(\text{II}) + E_{\text{Interaction}} \quad (1)$$

where E(I) and E(II) are the regions I and II energy, and $E_{\text{Interaction}}$ is the interaction energy of the two regions. By judiciously selecting a region which contains the chemically relevant atoms, a high-level quantum mechanical (QM) method is used to obtain E(I), and a cheaper computational method is used to compute E(II) and $E_{\text{Interaction}}$. Morokuma and co-workers have developed a particularly useful hybrid energy method called our own N-layered integrated molecular orbital and molecular mechanics (ONIOM).[17−23] This method is obtained by using the following definition of the interaction energy:

$$E_{\text{Interaction}} = E_{\text{LL}}(\text{I} + \text{II}) - E_{\text{LL}}(\text{I}) - E_{\text{LL}}(\text{II}) \quad (2)$$

where the LL subscripts indicate that the low level of theory is used. The standard ONIOM energy is therefore obtained from the following expression:

$$E_{\text{ONIOM}} = E_{\text{RL}} - E_{\text{ML}} + E_{\text{MH}} \quad (3)$$

where E_{RL}, E_{ML}, and E_{MH} denote the real system: low-level energy, the model system: low-level energy, and the model

* Corresponding author. E-mail: kraghava@indiana.edu.

10.1021/ct1004164 © 2010 American Chemical Society
Published on Web 09/21/2010

Scheme 1. Schematic Illustration of the Model System Preparation Procedure[a]

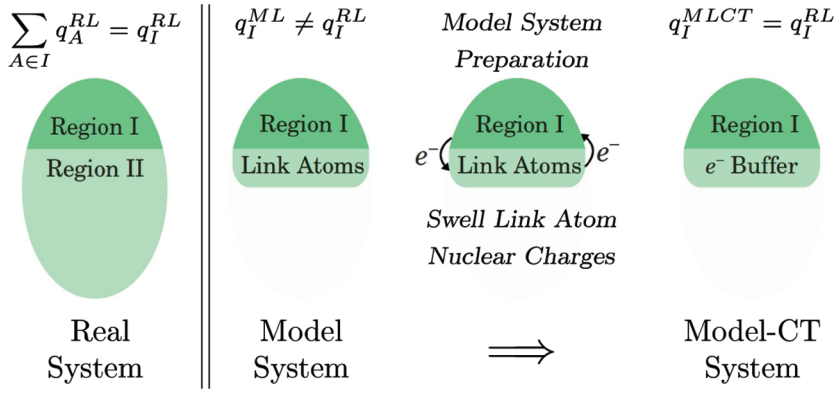

[a] Note that all of these steps are done with the low level of theory, and q_A denotes atomic charge for atom A, while q_I denotes regional charges for region I.

system: high-level energy, respectively. The real system, being the full, unpartitioned molecule, is composed of both regions I and II. The model system, however, consists of only region I with the addition of link atoms which cap "dangling bonds" created from severed covalent bonds. This type of energy expression allows one to couple different computational chemistry methods without modification.

Despite its success, the ONIOM truncation of the model system can impose some artificial effects. While all energetic contributions (coulomb, exchange, charge-transfer, etc.) are fully included via the E_{RL} subcalculation, they are done so only at the low level of theory. Difficulties may arise when the link atoms have different electron donating/accepting properties from the region II atoms. This can generate a significantly different amount of electron density in region I of the model system. In such a case, the high-level correction ($E_{MH} - E_{ML}$) is performed on a model system, which is either partially oxidized or reduced relative to the untruncated system. To treat this problem, one would need to effectively change the number of electrons to achieve a fractional charge in region I. In this direction, Merz and co-workers[24] have developed an approach to match chemical potentials of different regions in a divide and conquer method[25,26] by transferring charge from one region to another. While this was successfully done to couple density functional theory (DFT) and semiempirical methods, it is not clear whether this can be easily extended to post-self-consistent field (SCF) methods. Lin and co-workers have also addressed this problem in the context of quantum mechanical/molecular mechanical (QM/MM) methods.[27] In this approach, the fractional number of electrons is obtained by taking an ensemble average of integer charge states, whose weights are determined by the equalization of chemical potentials. Another hybrid method which also has the ability to describe some charge transfer from one region to the next is the generalized hybrid orbital (GHO) method of Gao and co-workers,[28−30] which has also found use in computing the QM units in biomolecular application of the X-Pol method.[31] Other workers have also treated the problem of cross-system charge redistribution, though in other contexts.[32−34]

In this paper, we provide an efficient method to include charge redistribution across regional boundaries in an ONIOM QM:QM calculation to reduce the unwanted electronic effects from truncation of the model system. This is done by means of a model system preparation step which provides a general approach to improving the standard ONIOM method.

2. Methods

In Scheme 1, we present a schematic illustration of the currently presented method in which we optimize the model system to minimize the electronic differences between the RL and ML subcalculations. To begin, the real system is partitioned into a chemically active region I and inactive region II. By summing the atomic charges over the atoms in region I, we obtain the region I charge at the low level of theory, q_I^{RL}. Similarly for the ML subcalculation, the region I charge, q_I^{ML}, is obtained by summing the atomic charges from the ML calculation, which are in region I (i.e., all but the link atom charges). Generally

$$q_I^{RL} \neq q_I^{ML} \tag{4}$$

and thus the amount of region I charge in the model system is not the same as that in the real system. As shown in the third column of Scheme 1, we swell (or diminish) the nuclear charges on the link atoms to pull (or push) electron density out of (or into) region I. The magnitude of the resulting link atom nuclear charges is chosen such that the following becomes true:

$$q_I^{RL} = q_I^{MLCT} \tag{5}$$

where q_I^{MLCT} denotes the region I charge from the low-level model CT calculation. Eq 5 is satisfied by iteratively optimizing the link-atom nuclear charges and, in practice, requires around 4−5 ML subcalculations to obtain convergence to $10^{-5}e$. Due to the relatively low cost of the ML calculation, this can be done without significantly increasing the overall computational effort. While the region I charge can be defined with any population analysis, we have chosen to use Löwdin charges[35] due to their computational simplicity and proven performance for use in other applications.[36,37] Later in the text we provide a performance comparison of a few commonly used population analyses.

Scheme 2. Flow Chart of an ONIOM-CT Calculation

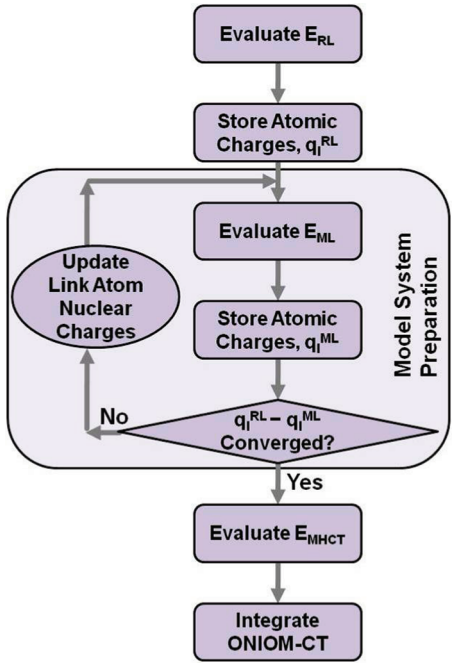

Once the optimal link-atom nuclear charges are obtained for the MLCT subcalculation, the MHCT subcalculation is then performed using the same link-atom nuclear charges with no further buffer region optimization. The ONIOM-CT energy expression is then given as

$$E_{\mathrm{ONIOM-CT}} = E_{\mathrm{RL}} - E_{\mathrm{MLCT}} + E_{\mathrm{MHCT}} \qquad (6)$$

where E_{MLCT} and E_{MHCT} denote the model CT energies with the low and high levels of theory, respectively. Note that the only difference between eqs 3 and 6 is that the model system has link atoms with modified nuclear charges. The individual steps of the ONIOM-CT calulation are shown in Scheme 2. We plan to make available a simple utility program, compatible with both Gaussian 03 and 09,[38,39] to facilite the computation of the ONIOM-CT energy.

Although we have defined the buffer region as the link atoms in this paper, the buffer region could also be chosen to include entire functional groups as well. Clearly, one would need to choose a different buffer region to describe charge-transfer effects for nonbonded model systems (i.e., no link atoms). However, the scaling procedure for the nuclear charges in such cases is not unique and has to be defined carefully. Just as the standard ONIOM approach requires model and real system definitions, the ONIOM-CT method requires model system, real system, and buffer region definitions. In future work, we will investigate the effect of different buffer region choices. While we currently only consider QM:QM models, it may be possible to perform an ONIOM-CT calculation with a MM low level (ONIOM-CT QM:MM) by using a polarizable force field to obtain the region I charges $q_{\mathrm{I}}^{\mathrm{RL}}$ and $q_{\mathrm{I}}^{\mathrm{ML}}$. We plan to investigate the viability of such an approach in the future.

3. Results

To assess the performance of the ONIOM-CT method, we have carried out a set of calculations for a representative test set of 20 chemical reactions using several different combinations of high and low levels of theory. The test set is listed in Table 1 and includes not only different types of reactions but also multiple electron-donating/-accepting properties of the region II subsystem (X = F and CH_3). The different high:low combinations, which are listed in Table 2, are chosen to highlight some of the effects of choosing combinations with varying disparities both in electron correlation (MP2:HF, B3LYP:B3LYP, MP2:B3LYP, and B3LYP:HF) and in basis set size (6-311+G(d,p):3-21G and 6-31+G(d):3-21G). Note that for the low level of theory, only the 3-21G basis set has been considered in this study. Since the regional charges are obtained from a population analysis of the low-level subcalculations, we have chosen to use a small low-level basis set to avoid the known problems associated with performing Mulliken and Löwdin population analyses with large basis sets.[40]

In Table 3, we provide the results for the full test set of reactions using each high:low combination listed in Table 2. Each quantity reported (e.g., mean absolute deviation (MAD), standard deviation, etc.) is given for each high:low combination with the averaged value given at the bottom. Throughout this paper, a deviation is defined as the difference between reaction energies obtained from the real high calculations and those from the ONIOM or ONIOM-CT calculations. Therefore, a zero deviation would indicate that the ONIOM or ONIOM-CT method produced a reaction

Table 1. Test Set of Reactions[a]

	Deprotonation		
1)	X_3C-≀≀-$CH_2OH_2^+$	⟶	X_3C-≀≀-$CH_2OH + H^+$
2)	X_3C-≀≀-CH_2OH	⟶	X_3C-≀≀-$CH_2O^- + H^+$
3)	X_3C-≀≀-$CH_2NH_3^+$	⟶	X_3C-≀≀-$CH_2NH_2 + H^+$
4)	X_3C-≀≀-CH_2NH_2	⟶	X_3C-≀≀-$CH_2NH^- + H^+$
5)	X_3C-≀≀-$COOH$	⟶	X_3C-≀≀-$COO^- + H^+$
	H-Abstraction		
6)	X_3C-≀≀-CH_2OH	⟶	X_3C-≀≀-$CH_2O^\bullet + H^\bullet$
7)	X_3C-≀≀-CH_2NH_2	⟶	X_3C-≀≀-$CH_2NH^\bullet + H^\bullet$
	Electron Affinity		
8)	X_3C-≀≀-CH_2O^-	⟶	X_3C-≀≀-$CH_2O^\bullet + e^-$
9)	X_3C-≀≀-CH_2NH^-	⟶	X_3C-≀≀-$CH_2NH^\bullet + e^-$
	S_N2 Reactions		
10)	X_3C-≀≀-$CH_2F + Cl^-$	⟶	X_3C-≀≀-$CH_2Cl + F^-$

[a] All 20 reactions have been carried out with X = F and CH_3. Location of ONIOM system partition is denoted by wavy lines.

Table 2. List of the Eight Combinations of High and Low Levels of Theory Used Throughout This Paper

entry	high level	:	low level
1a	MP2/6-311+G(d,p)	:	HF/3-21G
1b	MP2/6-31+G(d)	:	HF/3-21G
2a	B3LYP/6-311+G(d,p)	:	B3LYP/3-21G
2b	B3LYP/6-31+G(d)	:	B3LYP/3-21G
3a	MP2/6-311+G(d,p)	:	B3LYP/3-21G
3b	MP2/6-31+G(d)	:	B3LYP/3-21G
4a	B3LYP/6-311+G(d,p)	:	HF/3-21G
4b	B3LYP/6-31+G(d)	:	HF/3-21G

Table 3. Comparison of the Performance of the ONIOM and ONIOM-CT Methods[a]

	MAD		standard deviation		max deviation		MAD(X = F)		MAD(X = CH_3)	
high:low	ONIOM	ONIOM-CT	ONIOM	ONIOM-CT	ONIOM	ONIOM-CT	ONIOM	ONIOM-CT	ONIOM	ONIOM-CT
1a	3.26	1.58	3.99	2.14	6.65	5.45	3.90	1.83	2.62	1.34
1b	2.96	1.40	3.59	1.85	5.64	4.55	3.13	1.35	2.79	1.44
2a	3.80	2.77	5.67	3.51	11.77	6.67	1.45	2.01	6.15	3.53
2b	3.72	2.33	5.61	2.92	11.71	5.49	1.37	2.38	6.07	2.28
3a	3.70	2.36	5.29	3.09	10.86	7.06	1.87	3.00	5.53	1.73
3b	3.63	3.10	5.48	4.09	11.72	8.96	1.45	4.50	5.80	1.71
4a	3.49	2.34	4.14	2.75	6.71	4.78	3.53	2.34	3.46	2.33
4b	3.49	1.98	4.13	2.39	6.62	4.89	3.60	2.15	3.38	1.80
average	**3.51**	**2.23**	**4.74**	**2.84**	**8.96**	**5.98**	**2.54**	**2.45**	**4.48**	**2.02**

[a] Mean absolute deviation is MAD. MAD(X = F) indicates the MAD for the subset of reactions for which X = F. MAD(X = CH_3) indicates the MAD for the subset of reactions for which X = CH_3. Units are in kcal/mol.

energy identical to that of the high level of theory on the real system.

By inspection of the overall mean absolute deviations (MAD's) in the first two columns in Table 3, it is clear that the ONIOM-CT method provides significant overall improvements over the standard ONIOM method. While it is notable that the mean absolute deviation (MAD) for all 160 data points is reduced from 3.51 to 2.23 kcal/mol, it is especially encouraging to see that for every high:low combination the ONIOM-CT method provides significant improvements, at times reducing the MAD by over 50%.

The inclusion of charge redistibution during the model system preparation step not only reduces the MAD but also makes the performance of the ONIOM-CT method more reliable, as suggested by the significantly lower standard deviations of the ONIOM-CT method. For each high:low combination the standard deviation is significantly decreased with the averaged standard deviations being 4.74 and 2.84 kcal/mol for the ONIOM and ONIOM-CT methods, respectively. Also providing an indication of reliability, the maximum deviation for each high:low combination is also decreased with improvements of up to 6 kcal/mol with high:low 2b.

By separating the test set into two subsets, X = F and CH_3, it is observed that the accuracy with which the standard ONIOM method treats these two groups is quite uneven. Using the ONIOM method, the X = F reactions have an overall MAD of only 2.54 kcal/mol, while the analogous reactions with X = CH_3 have a MAD of 4.48 kcal/mol. Use of the ONIOM-CT method reduces the performance discrepancy between the two subsets with MAD's of 2.45 and 2.02 kcal/mol for the X = F and CH_3 reactions, respectively. These are listed in the last 4 columns of Table 3.

3.1. Effect on Region I Density. To demonstrate the physical effect of the model system preparation, we provide in Figure 1 a density difference plot of the model system densities for both $F_3C-//-COOH$ and $(CH_3)_3C-//-COOH$ molecules. Here, the density of the MLCT subsystem (ρ^{MLCT}) is obtained from the low-level calculation on the model system with the optimized link-atom nuclear charges, while the density of the ML subsystem (ρ^{ML}) is obtained from the low-level calculation on the model system before optimization (i.e., link-atom nuclear charges = 1). The density difference ($\rho^{MLCT} - \rho^{ML}$) is shown with the black and gray surfaces representing negative and positive density changes, respectively. To identify the locations of all the atomic centers, the bare molecules are given in the top of the figure, with the link-atom position shown as a translucent center. The ONIOM-CT method treats the link-atoms as a charge buffer region where density is either pushed out of or pulled into.

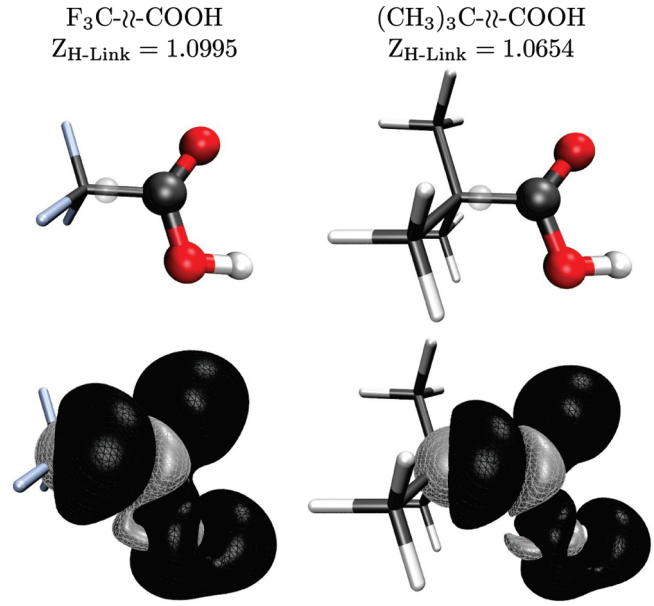

Figure 1. Change in density due to the model system preparation step, $\rho^{MLCT} - \rho^{ML}$. Black and gray surfaces represent negative and positive density changes, respectively. Isovalue = 0.0002. Translucent spheres indicate location of hydrogen link atoms. $Z_{H\text{-}Link}$ is the optimized value of the link-atom nuclear charge.

The effect on these two molecules is quite clear. As evident by the large amount of negative change in density around the oxygens, there is an overall transfer of negative charge out of region I into the buffer region. While both molecules show a qualitatively similar effect, the amount of charge redistributed is noticeably greater in $F_3C-//-COOH$. As F is a stronger electron acceptor than CH_3, this difference between the two molecules is consistent with what would be expected based on chemical intuition. The optimized link-atom nuclear charges giving rise to this transfer of density are 1.100 and 1.065 for $F_3C-//-COOH$ and $(CH_3)C-//-COOH$, respectively.

3.2. Dependence on Population Analysis. The nonexistence of physical observables corresponding to chemical

Table 4. Comparison of the ONIOM-CT Method Using Either Löwdin, Mulliken, or Hirshfeld Population Analysis to Define the Region I Charges[a]

		ONIOM-CT		
reaction type	ONIOM	Löwdin	Mulliken	Hirshfeld
deprotonation	3.83	2.24	2.62	2.86
H abstraction	0.52	1.04	1.84	1.14
electron affinity	5.71	3.12	4.46	3.81
S_N2	3.46	2.83	2.75	2.99
X = F	2.54	2.45	3.33	2.82
X = Me	4.48	2.02	2.36	2.62
σ (std dev)	4.74	2.84	3.68	3.42
overall MAD	**3.51**	**2.23**	**2.84**	**2.72**

[a] Results are given for all 160 reaction energies and are in kcal/mol.

quantities, such as the atomic charge, imposes a certain degree of arbitrariness upon any model which makes use of them. In the previous section, we report results for the ONIOM-CT method using Löwdin charges to define the region I charges, q_I^{RL} and q_I^{MLCT}, which are used during the model system preparation step. However, while Löwdin charges have been found to be favorable compared to other commonly used population analyses, benefit from their use is not obvious in this context, and thus we provide a comparison of the performance of a few different population analyses as used in the ONIOM-CT method.

In Table 4 we list the overall results (20 reactions and 8 high:low combinations) for the standard ONIOM and the ONIOM-CT methods using either Löwdin, Mulliken,[41] or Hirshfeld charges[42] during the model system preparation step.

From an inspection of the overall MAD's and average standard deviations for the different ONIOM-CT results, use of Löwdin charges provides the best performance, with a MAD of only 2.23 kcal/mol compared to 2.84 and 2.72 kcal/mol for Mulliken and Hirshfeld charges, respectively. Note however that while the performance does indeed have a dependence on the type of atomic charges used, all three population analyses provide significant improvements over the standard ONIOM-CT method in both the overall MAD and the standard deviations.

In all the examples listed in Table 2, we have only used the 3-21G basis set in the low level to avoid potential problems associated with using charges from a density matrix-based population analysis with large basis sets. We also carried out a few additional calculations to test the stability of the ONIOM-CT energy with increasing the low-level basis set size. Using the high:low combination MP2/6-311+G(d,p):HF/6-311+G(d,p) as an example, we found a decrease in the performance of the ONIOM-CT method compared to the standard ONIOM method with MADs of 2.53 and 1.62 kcal/mol for ONIOM-CT and ONIOM, respectively. Based on these results, it is suggested that large basis sets in the low level of theory be used with caution. If large low-level basis sets are required, then it may be advantageous to first project the associated wave functions onto a minimal basis set prior to performing the population analysis. We plan to investigate this carefully in future works.

4. Conclusions

In this paper, we have provided an inexpensive approach to describing inter-region charge-transfer effects in an ONIOM formalism. In this method, link-atom centers are treated as an electron buffer region, and their nuclear charges are swelled or diminished to transfer density into or out of the buffer region until the model system region I charge is identical to the real system region I charge.

To assess the performance of the ONIOM-CT method, we have performed calculations on a test set of 20 different reaction energies using 8 different combinations of high and low levels of theory. From these results it was found that for each high:low pair, the ONIOM-CT method provided significantly improved results as compared to the standard ONIOM method. For two of the high:low pairs, ONIOM-CT was found to be over 50% more accurate that ONIOM. Averaging over all high:low pairs, the overall MAD was decreased from 3.51 to 2.23 kcal/mol. In addition to improvements in accuracy, ONIOM-CT also provided precision gains as reflected by the greatly reduced standard and maximum deviations.

We have also performed a comparative assessment of using different population analyses in the model system preparation step. Among the Löwdin, Mulliken, and Hirshfeld atomic charge definitions, use of Löwdin charges provided the greatest improvements in both accuracy and precision over the standard ONIOM method.

While the focus of this work was to include the effects of charge redistribution from one ONIOM layer to another, the model system preparation step used in the ONIOM-CT method provides a general framework in which one may improve the ONIOM method.

Future plans include the development of an efficient procedure for obtaining gradients, coupling of the model system preparation step with our previous work on electronic embedding,[36,43,44] and also generalizing the definition of the buffer region to extend beyond link atoms.

Acknowledgment. This work was supported by an National Science Foundation grant, CHE-0911454, at Indiana University. The authors would like to thank Dr. Mike Frisch for helpful suggestions related to this work and Dr. Hrant Hratchian for useful comments on the manuscript.

References

(1) Curtiss, L. A.; Redfern, P. C.; Raghavachari, K. *J. Chem. Phys.* **2007**, *126*, 084108−084119.

(2) DeYonker, N. J.; Cundari, T. R.; Wilson, A. K. *J. Chem. Phys.* **2006**, *124*, 114104.

(3) Boese, A. D.; Oren, M.; Atasoylu, O.; Martin, J. M. L.; Kallay, M.; Gauss, J. *J. Chem. Phys.* **2004**, *120*, 4129–4141.

(4) Ochterski, J. W.; Petersson, G. A.; Montgomery, J. A., Jr. *J. Chem. Phys.* **1996**, *104*, 2598.

(5) Karton, A.; Rabinovich, E.; Martin, J. M.; Ruscic, B. *J. Chem. Phys.* **2006**, *125*, 144108.

(6) Tajti, A.; Szalay, P.; Csaszar, A.; Kallay, M.; Gauss, J.; Valeev, E.; Flowers, B.; Vazquez, J.; Stanton, J. *J. Chem. Phys.* **2004**, *121*, 11599.

(7) Warshel, A.; Levitt, M. *J. Mol. Biol.* **1976**, *103*, 227–249.

(8) Singh, U. C.; Kollman, P. A. *J. Comput. Chem.* **1986**, *7*, 718–730.

(9) Field, M. J.; Bash, P. A.; Karplus, M. *J. Comput. Chem.* **1990**, *11*, 700–733.

(10) Aqvist, J.; Warshel, A. *Chem. Rev.* **1993**, *93*, 2523–2544.

(11) Maseras, F.; Morokuma, K. *J. Comput. Chem.* **1995**, *16*, 1170–1179.

(12) Mordasini, T.; Thiel, W. *Chimia* **1998**, *52*, 288–291.

(13) Monard, G.; Merz, K. M. *Acc. Chem. Res.* **1999**, *32*, 904–911.

(14) Gao, J. L.; Truhlar, D. G. *Annu. Rev. Phys. Chem.* **2002**, *53*, 467–505.

(15) Field, M. J. *J. Comput. Chem.* **2002**, *23*, 48–58.

(16) Lin, H.; Truhlar, D. G. *Theor. Chem. Acc.* **2007**, *117*, 185–199.

(17) Humbel, S.; Sieber, S.; Morokuma, K. *J. Chem. Phys.* **1996**, *105*, 1959–1967.

(18) Svensson, M.; Humbel, S.; Froese, R.; Matsubara, T.; Sieber, S.; Morokuma, K. *J. Phys. Chem.* **1996**, *100*, 19357–19363.

(19) Karadakov, P. B.; Morokuma, K. *Chem. Phys. Lett.* **2000**, *317*, 589–596.

(20) Vreven, T.; Morokuma, K. *J. Comput. Chem.* **2000**, *21*, 1419–1432.

(21) Vreven, T.; Mennucci, B.; da Silva, C.; Morokuma, K.; Tomasi, J. *J. Chem. Phys.* **2001**, *115*, 62–72.

(22) Vreven, T.; Morokuma, K. *Theor. Chem. Acc.* **2003**, *109*, 125–132.

(23) Rega, N.; Iyengar, S.; Voth, G.; Schlegel, H.; Vreven, T.; Frisch, M. *J. Phys. Chem. B* **2004**, *108*, 4210–4220.

(24) Gogonea, V.; Westerhoff, L. M.; Merz, K. M. *J. Chem. Phys.* **2000**, *113*, 5604.

(25) Yang, W.; Lee, T. *J. Chem. Phys.* **1995**, *103*, 5674.

(26) Dixon, S. L.; Merz, K. M. *J. Chem. Phys.* **1996**, *104*, 6643.

(27) Zhang, Y.; Lin, H. *J. Chem. Theor. Comp.* **2008**, *4*, 414–425.

(28) Gao, J. L.; Amara, P.; Alhambra, C.; Field, M. J. *J. Phys. Chem. A* **1998**, *102*, 4714–4721.

(29) Pu, J. Z.; Gao, G. L.; Truhlar, D. G. *J. Phys. Chem. A* **2004**, *108*, 632–650.

(30) Pu, J. Z.; Gao, J. L.; Truhlar, D. G. *Chem. Phys. Chem.* **2005**, *6*, 1853–1865.

(31) Xie, W. S.; Gao, J. L. *J. Comp. Theor. Comp.* **2007**, *3*, 1890–1900.

(32) Aviram, A.; Ratner, M. A. *Chem. Phys. Lett.* **1974**, *29*, 277–283.

(33) Nitzan, A.; Ratner, M. A. *Science* **2003**, *300*, 1384–1389.

(34) Pacheco, A.; Iyengar, S. S. *J. Chem. Phys.* **2010**, *133*, 044106.

(35) Löwdin, P. O. *Adv. Quantum Chem.* **1970**, *5*, 185–199.

(36) Mayhall, N. J.; Raghavachari, K.; Hratchian, H. P. *J. Chem. Phys.* **2010**, *132*, 114107.

(37) Wu, Q.; Van Voorhis, T. *J. Phys. Chem. A* **2006**, *110*, 9212.

(38) Frisch, M. J.; Trucks, G. W.; Schlegel, H. B.; Scuseria, G. E.; Robb, M. A.; Cheeseman, J. R.; Montgomery, J. A., Jr.; Vreven, T.; Kudin, K. N.; Burant, J. C.; Millam, J. M.; Iyengar, S. S.; Tomasi, J.; Barone, V.; Mennucci, B.; Cossi, M.; Scalmani, G.; Rega, N.; Petersson, G. A.; Nakatsuji, H.; Hada, M.; Ehara, M.; Toyota, K.; Fukuda, R.; Hasegawa, J.; Ishida, M.; Nakajima, T.; Honda, Y.; Kitao, O.; Nakai, H.; Klene, M.; Li, X.; Knox, J. E.; Hratchian, H. P.; Cross, J. B.; Bakken, V.; Adamo, C.; Jaramillo, J.; Gomperts, R.; Stratmann, R. E.; Yazyev, O.; Austin, A. J.; Cammi, R.; Pomelli, C.; Ochterski, J. W.; Ayala, P. Y.; Morokuma, K.; Voth, G. A.; Salvador, P.; Dannenberg, J. J.; Zakrzewski, V. G.; Dapprich, S.; Daniels, A. D.; Strain, M. C.; Farkas, O.; Malick, D. K.; Rabuck, A. D.; Raghavachari, K.; Foresman, J. B.; Ortiz, J. V.; Cui, Q.; Baboul, A. G.; Clifford, S.; Cioslowski, J.; Stefanov, B. B.; Liu, G.; Liashenko, A.; Piskorz, P.; Komaromi, I.; Martin, R. L.; Fox, D. J.; Keith, T.; Al-Laham, M. A.; Peng, C. Y.; Nanayakkara, A.; Challacombe, M.; Gill, P. M. W.; Johnson, B.; Chen, W.; Wong, M. W.; Gonzalez, C.; Pople, J. A. *Gaussian 03*, Revision C.02; Gaussian, Inc.: Wallingford, CT, 2004.

(39) Frisch, M. J.; Trucks, G. W.; Schlegel, H. B.; Scuseria, G. E.; Robb, M. A.; Cheeseman, J. R.; Scalmani, G.; Barone, V.; Mennucci, B.; Petersson, G. A.; Nakatsuji, H.; Caricato, M.; Li, X.; Hratchian, H. P.; Izmaylov, A. F.; Bloino, J.; Zheng, G.; Sonnenberg, J. L.; Hada, M.; Ehara, M.; Toyota, K.; Fukuda, R.; Hasegawa, J.; Ishida, M.; Nakajima, T.; Honda, Y.; Kitao, O.; Nakai, H.; Vreven, T.; Montgomery, J. A., Jr.; Peralta, J. E.; Ogliaro, F.; Bearpark, M.; Heyd, J. J.; Brothers, E.; Kudin, K. N.; Staroverov, V. N.; Kobayashi, R.; Normand, J.; Raghavachari, K.; Rendell, A.; Burant, J. C.; Iyengar, S. S.; Tomasi, J.; Cossi, M.; Rega, N.; Millam, J. M.; Klene, M.; Knox, J. E.; Cross, J. B.; Bakken, V.; Adamo, C.; Jaramillo, J.; Gomperts, R.; Stratmann, R. E.; Yazyev, O.; Austin, A. J.; Cammi, R.; Pomelli, C.; Ochterski, J. W.; Martin, R. L.; Morokuma, K.; Zakrzewski, V. G.; Voth, G. A.; Salvador, P.; Dannenberg, J. J.; Dapprich, S.; Daniels, A. D.; Farkas, Ã.; Foresman, J. B.; Ortiz, J. V.; Cioslowski, J.; Fox, D. J. *Gaussian 09*, Revision A.1; Gaussian Inc.: Wallingford, CT, 2009.

(40) Jensen, F. *Introduction to Computational Chemistry*, 2nd ed.; John Wiley & Sons: Chichester, England, 2007; pp 293−296.

(41) Mulliken, R. S. *J. Chem. Phys.* **1962**, *36*, 3428.

(42) Hirshfeld, F. L. *Theor. Chem. Acc.* **1977**, *44*, 129.

(43) Hratchian, H. P.; Parandekar, P. V.; Raghavachari, K.; Frisch, M. J.; Vreven, T. *J. Chem. Phys.* **2008**, *128*, 034107.

(44) Parandekar, P. V.; Hratchian, H. P.; Raghavachari, K. *J. Chem. Phys.* **2008**, *129*, 145101.

CT1004164